



This discussion paper is/has been under review for the journal Atmospheric Measurement Techniques (AMT). Please refer to the corresponding final paper in AMT if available.

# Aircraft based four-channel thermal dissociation laser induced fluorescence instrument for simultaneous measurements of NO<sub>2</sub>, total peroxy nitrate, total alkyl nitrate, and HNO<sub>3</sub>

P. Di Carlo<sup>1,2</sup>, E. Aruffo<sup>1,2</sup>, M. Busilacchio<sup>1,2</sup>, F. Giammaria<sup>2</sup>,  
C. Dari-Salisburgo<sup>1,2</sup>, F. Biancofiore<sup>1,2</sup>, G. Visconti<sup>1,2</sup>, J. Lee<sup>3</sup>, S. Moller<sup>3</sup>,  
C. E. Reeves<sup>4</sup>, S. Bauguitte<sup>5</sup>, G. Forster<sup>4</sup>, R. L. Jones<sup>6</sup>, and B. Ouyang<sup>6</sup>

<sup>1</sup>Center of Excellence CETEMPS, Universita' degli studi di L'Aquila, Via Vetoio, 67010 Coppito, L'Aquila, Italy

<sup>2</sup>Dipartimento di Scienze Fisiche e Chimiche, Universita' degli studi di L'Aquila, Via Vetoio, 67010 Coppito, L'Aquila, Italy

<sup>3</sup>Department of Chemistry, University of York, York, UK

<sup>4</sup>School of Environmental Sciences, University of East Anglia, Norwich, UK

<sup>5</sup>Facility for Airborne Atmospheric Measurements, Bedfordshire, UK

<sup>6</sup>Department of Chemistry, University of Cambridge, Cambridgeshire, UK

[Title Page](#)

[Abstract](#)

[Introduction](#)

[Conclusions](#)

[References](#)

[Tables](#)

[Figures](#)

◀

▶

[Back](#)

[Close](#)

[Full Screen / Esc](#)

[Printer-friendly Version](#)

[Interactive Discussion](#)



Received: 21 November 2012 – Accepted: 1 December 2012 – Published: 6 December 2012

Correspondence to: P. Di Carlo (piero.dicarlo@aquila.infn.it)

Published by Copernicus Publications on behalf of the European Geosciences Union.

AMTD

5, 8759–8787, 2012

---

## Aircraft TD-LIF

P. Di Carlo et al.

---

[Title Page](#)

[Abstract](#)

[Introduction](#)

[Conclusions](#)

[References](#)

[Tables](#)

[Figures](#)

◀

▶

◀

▶

[Back](#)

[Close](#)

[Full Screen / Esc](#)

[Printer-friendly Version](#)

[Interactive Discussion](#)



## Abstract

A four-channel thermal dissociation laser induced fluorescence (TD-LIF) instrument has been developed for simultaneous measurements of nitrogen dioxide ( $\text{NO}_2$ ), total peroxy nitrate ( $\sum\text{PNs}$ ), total alkyl nitrate ( $\sum\text{ANs}$ ) and nitric acid ( $\text{HNO}_3$ ).  $\text{NO}_2$  is measured directly by LIF at 532 nm, whereas organic nitrates and nitric acid are thermally dissociated at distinct temperatures in the inlet to form  $\text{NO}_2$ , which is then measured by LIF. The concentrations of each dissociated species are derived by the differences in measured  $\text{NO}_2$  relative to the reference colder inlet channel. The TD-LIF was adapted to fly on board the UK Facility for Airborne Atmospheric Measurements (FAAM) BAe 146-301 atmospheric research aircraft in summer 2010, and to date has successfully flown in five field campaigns. This paper reports novel improvements in the TD-LIF instrumentations including: (1) the use of a single wavelength laser, which makes the system compact and relatively cheap; (2) the use of a single beam laser that allows easy alignment and optical stability against the vibrational aircraft environment and (3) the optical assembly of four detection cells that allow simultaneous and fast (time resolution up to 0.1 s) measurements of  $\text{NO}_2$ ,  $\sum\text{PNs}$ ,  $\sum\text{ANs}$  and  $\text{HNO}_3$ . Laboratory-generated mixtures of PNs, ANs and  $\text{HNO}_3$  in zero air are converted into  $\text{NO}_2$  and used to fix the dissociation temperatures of each heated inlet, to test the selectivity of the instrument and potential interferences due to recombination reactions of the dissociated products. The effectiveness of the TD-LIF was demonstrated during the RONOCO aircraft campaign (summer 2010). A chemiluminescence system that was measuring  $\text{NO}_2$  and a broadband cavity enhanced absorption spectrometer (BBCEAS) that was measuring one of the PNs ( $\text{N}_2\text{O}_5$ ) were installed on the same aircraft during the campaign. The in-flight intercomparison of the new TD-LIF with the chemiluminescence system for  $\text{NO}_2$  measurements and the intercomparison between  $\sum\text{PNs}$  measured by the TD-LIF and  $\text{N}_2\text{O}_5$  by the BBCEAS are used to assess the performance of the TD-LIF.

5 532 nm, whereas organic nitrates and nitric acid are thermally  
dissociated at distinct temperatures in the inlet to form  $\text{NO}_2$ , which is then measured by  
LIF. The concentrations of each dissociated species are derived by the differences in  
measured  $\text{NO}_2$  relative to the reference colder inlet channel. The TD-LIF was adapted  
to fly on board the UK Facility for Airborne Atmospheric Measurements (FAAM) BAe  
10 146-301 atmospheric research aircraft in summer 2010, and to date has successfully  
flown in five field campaigns. This paper reports novel improvements in the TD-LIF  
instrumentations including: (1) the use of a single wavelength laser, which makes the  
system compact and relatively cheap; (2) the use of a single beam laser that allows  
easy alignment and optical stability against the vibrational aircraft environment and  
15 (3) the optical assembly of four detection cells that allow simultaneous and fast (time  
resolution up to 0.1 s) measurements of  $\text{NO}_2$ ,  $\sum\text{PNs}$ ,  $\sum\text{ANs}$  and  $\text{HNO}_3$ . Laboratory-  
generated mixtures of PNs, ANs and  $\text{HNO}_3$  in zero air are converted into  $\text{NO}_2$  and used  
to fix the dissociation temperatures of each heated inlet, to test the selectivity of the  
20 instrument and potential interferences due to recombination reactions of the dissociated  
products. The effectiveness of the TD-LIF was demonstrated during the RONOCO air-  
craft campaign (summer 2010). A chemiluminescence system that was measuring  $\text{NO}_2$  and a  
broadband cavity enhanced absorption spectrometer (BBCEAS) that was mea-  
suring one of the PNs ( $\text{N}_2\text{O}_5$ ) were installed on the same aircraft during the campaign.  
The in-flight intercomparison of the new TD-LIF with the chemiluminescence system for  
25  $\text{NO}_2$  measurements and the intercomparison between  $\sum\text{PNs}$  measured by the TD-LIF  
and  $\text{N}_2\text{O}_5$  by the BBCEAS are used to assess the performance of the TD-LIF.

[Title Page](#)

[Abstract](#)

[Introduction](#)

[Conclusions](#)

[References](#)

[Tables](#)

[Figures](#)

◀

▶

◀

▶

[Back](#)

[Close](#)

[Full Screen / Esc](#)

[Printer-friendly Version](#)

[Interactive Discussion](#)



# 1 Introduction

Atmospheric peroxy nitrates (PNs or  $\text{RO}_2\text{NO}_2$ ), alkyl nitrates (ANs or  $\text{RONO}_2$ ) and nitric acid ( $\text{HNO}_3$ ) are high oxides of nitrogen formed as intermediate or final products in the oxidation chains of volatile organic compounds (VOC) that, in the presence of 5 nitrogen oxides ( $\text{NO}_x = \text{NO} + \text{NO}_2$ ), may produce ozone ( $\text{O}_3$ ). The main branch of the reaction between  $\text{RO}_2$  and NO produce  $\text{NO}_2$  which upon photolysis generates  $\text{O}_3$ , while a minor branch makes ANs; therefore the alkyl nitrate concentrations are generally considered as a good indication of ozone production. PNs are generated from the reaction of  $\text{RO}_2$  with  $\text{NO}_2$ , they are thermally unstable and their lifetime is strongly controlled by atmospheric temperature. Consequently, PNs are reservoirs of  $\text{NO}_x$  at low 10 temperature, releasing  $\text{NO}_x$  when temperature rises. This is one of the mechanisms for transporting  $\text{NO}_x$  from emission sites to remote places across long distance.  $\text{HNO}_3$  is one of the effective sinks for  $\text{NO}_x$  and for the main atmospheric oxidant hydroxyl radical ( $\text{OH} + \text{NO}_2 \rightarrow \text{HNO}_3$ ), owing to its high stability in the atmosphere.  $\text{HNO}_3$  is very 15 water soluble, whereas organic nitrates (PNs and ANs) are weakly water soluble. Despite the different characteristics PNs, ANs and  $\text{HNO}_3$  are important components of the total reactive nitrogen ( $\text{NO}_y = \text{NO} + \text{NO}_2 + \text{PN} + \text{AN} + \text{HNO}_3 + \text{NO}_3 + \text{N}_2\text{O}_5 + \text{HONO} + \text{other nitrates}$ ) and they may act as a sink or a reservoir of  $\text{NO}_x$ . Due to their tight connection with the production of a pollutant and greenhouse compound like  $\text{O}_3$ , organic nitrates 20 and  $\text{HNO}_3$  have been studied in detail in the recent years, but various aspects of their atmospheric chemistry are still not completely understood, for examples the products of the OH-initiated degradation of organic nitrate. In fact it is still uncertain if the reaction of organic nitrates with OH leads to a release of  $\text{NO}_x$ , retention of the nitrate group, or additional  $\text{NO}_x$  sequestration (Monks et al., 2009). The natural release of organic nitrates is also an area of uncertainty, in fact there are regions where the ocean seems 25 to be a source of ANs and others where it acts as a sink (Blake et al., 2003; Chuck et al., 2002).

[Title Page](#)[Abstract](#)[Introduction](#)[Conclusions](#)[References](#)[Tables](#)[Figures](#)[|◀](#)[▶|](#)[◀](#)[▶](#)[Back](#)[Close](#)[Full Screen / Esc](#)[Printer-friendly Version](#)[Interactive Discussion](#)

Individual organic nitrates have been measured with high sensitivity in several ground-based and aircraft campaigns, using gas chromatography (GC), which has the advantage of giving the concentrations of individual organic nitrates, but requires calibration for each of them. The time resolution is also quite low (Hao et al., 1994; Flocke et al., 2005; Reeves et al., 2007). GC thermal dissociation of organic nitrates followed by chemiluminescence detection of  $\text{NO}_2$  is a way to circumvent the need for calibration and to improve the time resolution of the GC up to 1 min (Hao et al., 1994; Marley et al., 2004). Thermal dissociation–chemical ionization mass spectrometry (TD-CIMS) technique has also been used to observe some organic nitrates like peroxyacetyl nitrate (PAN), peroxypropionyl nitrate (PPN), peroxymethacryloyl nitrate (MPAN), the sum of  $\text{N}_2\text{O}_5$  and  $\text{NO}_3$ , and  $\text{HNO}_3$  at high time resolution (less than 0.3 s), fast enough to retrieve their flux using the eddy covariance technique (Slusher et al., 2004; Turnipseed et al., 2006).

In the last decade a new approach has been proposed; this takes advantage of the fact that all compounds of the form  $\text{RO}_2\text{NO}_2$  have a similar thermal decomposition temperature into  $\text{NO}_2$  and that this temperature is significantly different from the dissociation temperature of all the species of the form  $\text{RONO}_2$  and both are distinct from that of  $\text{HNO}_3$  (Day et al., 2002). Cohen's group at the University of California, Berkeley has developed a system that heats atmospheric air at three separate temperatures to thermally dissociate total PNs ( $\sum\text{PNs}$ ), total ANs ( $\sum\text{ANs}$ ) and  $\text{HNO}_3$  into  $\text{NO}_2$ , whose concentration is measured by a laser induced fluorescence (LIF) system (Day et al., 2002). Although this method does not allow the quantification of individual organic nitrates, the division of the  $\text{NO}_y$  into 3 groups has been used to assess the role of  $\sum\text{ANs}$  in the  $\text{NO}_y$  budget. The sensitive measurements (ppt level) and high temporal resolution (<1 s) allow the measurement of organic nitrates at remote sites and in the free troposphere, and enable their fluxes to be estimated using the eddy covariance technique (Farmer and Cohen, 2008; Perring et al., 2009). More recently, this method has been applied using a similar scheme to thermally dissociate organic nitrates followed by different techniques to detect  $\text{NO}_2$  concentrations. A thermal dissociation-cavity

[Title Page](#)[Abstract](#)[Introduction](#)[Conclusions](#)[References](#)[Tables](#)[Figures](#)[|◀](#)[▶|](#)[◀](#)[▶](#)[Back](#)[Close](#)[Full Screen / Esc](#)[Printer-friendly Version](#)[Interactive Discussion](#)

ring-down spectrometer (TD-CRDS) has been successfully tested in the lab and during a field campaign by Osthoff's group at the University of Calgary with a similar detection limit and time resolution to Cohen's TD-LIF, with the potential advantage of not needing external calibration (Paul et al., 2009).

5 In this paper a new TD-LIF system for measurements of  $\text{NO}_2$ ,  $\sum\text{PNs}$ ,  $\sum\text{ANs}$  and  $\text{HNO}_3$  concentration on-board an atmospheric research aircraft is described. The TD-LIF uses an inlet at ambient temperature to directly measure ambient  $\text{NO}_2$ , and heated inlets to measure the abundance of  $\sum\text{PNs}$ ,  $\sum\text{ANs}$  and  $\text{HNO}_3$ . It is similar to that used by Cohen's group (Day et al., 2002) but in this work a simpler laser with a fixed wavelength is used to make the system easier to align, stable under in-flight vibrations and to supply enough power to be used in a series of 4 distinct cells to simultaneously measure  $\text{NO}_2$ ,  $\sum\text{PNs}$ ,  $\sum\text{ANs}$  and  $\text{HNO}_3$  with high time resolution. Results of laboratory tests to check the performance of the TD-LIF and to quantify possible interferences were also presented. Since the TD-LIF is included in the suite of the instruments on 10 board the Facility for Airborne Atmospheric Measurements (FAAM) BAe 146-301 research aircraft, and in one of the campaigns it was used concurrently with other systems, we are able to show in-flight measurements and comparisons with a couple of 15 different instruments that were measuring  $\text{NO}_2$  and  $\sum\text{PNs}$ .

## 2 The TD-LIF instrument

20 The TD-LIF uses the laser induced fluorescence technique with a single-wavelength laser, for direct detection of  $\text{NO}_2$ , which has previously been applied in ground-based systems (Matsumoto et al., 2001; Dari-Salisburgo et al., 2009). Organic nitrates and  $\text{HNO}_3$  are thermally dissociated allowing them to be detected as  $\text{NO}_2$  (Day et al., 2002; Paul et al., 2009). The optical layout and the inlet assembly are shown schematically 25 in Fig. 1.

[Title Page](#)

[Abstract](#)

[Introduction](#)

[Conclusions](#)

[References](#)

[Tables](#)

[Figures](#)

◀

▶

[Back](#)

[Close](#)

[Full Screen / Esc](#)

[Printer-friendly Version](#)

[Interactive Discussion](#)



## 2.1 Optical layout and LIF system

The light source is a pulsed YAG-laser (Spectra-Physics, model Navigator I) that emits light at 532 nm with a power of 3.8 W, a repetition rate of 15 kHz and 20 ns pulse-width. The laser beam is sent to the first cell (for ambient  $\text{NO}_2$  detection) using high reflectivity mirrors (> 99 % at 532 nm and 45°). The laser light that emerges from the  $\text{NO}_2$  cell is directed to the  $\sum\text{PNs}$  cell by another high reflectivity mirror; an identical optical scheme is used to steer the laser beam from the exit of the  $\sum\text{PNs}$  cell to the  $\sum\text{ANs}$  cell and finally to the  $\text{HNO}_3$  cell. All the cells are identical with a cubic core of 8 cm length and two arms on the opposite faces of the cube to hold a sequence of baffles to reduce the laser scattering. The walls of the cell, arms and baffles are coated with a low fluorescent optical black paint (MH2200, IIT Research Institute). All the cells are fixed on an optical table fitted in the middle of the FAAM rack to fly on board the BAe 146-301 research aircraft using anti-vibration mounts (Fig. 2). The laser head is attached below the optical table to be joined with the cells and to benefit from anti-vibration mounts. The air flow, ensured by a supercharger (Lysholm 3300) backed by a rotary pump (Leybold D25B), is perpendicular to the laser beam and the fluorescence emitted by excited  $\text{NO}_2$  molecules is collected perpendicular to both using a PMT (Hamamatsu, model 7421-50). To increase the photon collection efficiency, two lens (5 cm-diameter; 60 mm focal length and 10 mm focal length, respectively) are placed before the PMT and an aluminum coated concave mirror is mounted below the center of the cell to send fluorescent photons in the direction of the PMT (Dari-Salisburgo et al., 2009). Before the PMT a series of low fluorescence optical filters is used to separate fluorescent light from non-fluorescence photons that are collectively considered background: (1) two long pass filters (cut wavelengths: 620 and 640 nm, 25 mm diameter, transmission more than 85 % above 640 nm) and (2) two filters to reject the laser Rayleigh scatter (a razon 532 nm and a notch 532 nm filter of 25 mm diameter,  $10^6$  attenuation at 532 nm and transmission about 95 % above 532 nm) (Dari-Salisburgo et al., 2009). To further reduce the background, the photon detection is temporarily activated after each laser

[Title Page](#)[Abstract](#)[Introduction](#)[Conclusions](#)[References](#)[Tables](#)[Figures](#)[|◀](#)[▶|](#)[◀](#)[▶](#)[Back](#)[Close](#)[Full Screen / Esc](#)[Printer-friendly Version](#)[Interactive Discussion](#)

pulse for few  $\mu\text{s}$  and then deactivated until the end of the subsequent laser pulse (Dari-Salisburgo et al., 2009). The laser power is monitored with four photodiodes (UDT55) at the entrance of each cell.

## 2.2 Sampling and inlet system

5 Ambient air is sampled from a common rear-faced inlet (PFA tube of 120 cm, 6.4 mm OD and 3.8 mm ID) at a flow rate of  $\sim 8.4 \text{ L min}^{-1}$ . The air flow is split into four channels and passes through U-shaped quartz tubes (60 cm length, 6 mm OD, 3.8 mm ID). The first quartz tube is kept at ambient temperature and the sampled air goes to the first cell for ambient  $\text{NO}_2$  measurements, whereas the other three are heated at different temperatures to thermally dissociate  $\sum\text{PNs}$ ,  $\sum\text{ANs}$  and  $\text{HNO}_3$  into  $\text{NO}_2$ . Concentrations of the resultant  $\text{NO}_2$  are measured in the last three distinct cells. The air is heated using a 132 W wire (Watlow) coiled around the first 20 cm of the quartz tubes. Each tube temperature is monitored with a K-type thermocouple used also for the feedback of the power controller (STOM 1, United Automation) of the wire heater. The thermocouples 10 are fixed on the external surface of the quartz tubes in order not to perturb the sampled air, therefore their temperatures are different from the air temperatures inside the tubes and their settings are identified by sampling synthetic organic nitrates and  $\text{HNO}_3$  and scanning the heater temperatures to find those that guarantee the complete dissociation 15 of these species into  $\text{NO}_2$ . Figure 3 shows an example of the temperature scan while the TD-LIF was sampling synthetic PAN, ethyl nitrate and  $\text{HNO}_3$ . PAN was generated 20 in the laboratory by acetone photolysis at 285 nm in the presence of  $\text{O}_2$  and NO (Flocke et al., 2005); a dilute mixture of ethyl nitrate was generated using liquid ethyl nitrates (SelecLab Chemical, 5 % in ethanol), diluted and flushed with a small flow of zero air and finally  $\text{HNO}_3$  was generated by flowing zero air through a heated permeation tube (Kin-Tek) (McKinley and Merriman, 1980). The 3 distinct temperatures (150–250  $^{\circ}\text{C}$ ), (350–450  $^{\circ}\text{C}$ ) and above 550  $^{\circ}\text{C}$  when complete dissociation of  $\sum\text{PNs}$ ,  $\sum\text{ANs}$  25 and  $\text{HNO}_3$  take place are evident in Fig. 3. These setting temperatures may need to be re-adjusted upon changing the assembly of the heater wire and of the thermocouple,

[Title Page](#)[Abstract](#)[Introduction](#)[Conclusions](#)[References](#)[Tables](#)[Figures](#)[|◀](#)[▶|](#)[◀](#)[▶](#)[Back](#)[Close](#)[Full Screen / Esc](#)[Printer-friendly Version](#)[Interactive Discussion](#)

therefore they are indicative and must be checked periodically, and when parts (mainly the heater wire or the thermocouple) are replaced. Laboratory tests carried out to check the selectivity of the TD-LIF and for possible interferences are described in a dedicated section below.

5 The flow rate and the residence time through the quartz tube where the heater are mounted are  $2.1 \text{ L min}^{-1}$  and 30 ms, respectively. Sample air at the exit of the quartz tube undergoes a pressure drop of 93 % from ambient pressure to about 50 torr, passing through a pinhole. This pressure drop reduces the residence time of the sample gas between the heater region and the detection cell minimizing the occurrence of 10 recombination reactions. From the pinhole (after the quartz tube) and the detection cell, the sample air traverses a PFA tube of the same size as the inlet tube and about 100 cm long (residence time in this tube is 90 ms). This PFA tube delivers sample air to a stainless steel nozzle in the detection cell, where the pressure drops to about 4 torr. Considering that the residence time of the first part of the sampling tube (from the inlet 15 to the heaters) is 400 ms, the total residence time from the inlet to the detection cell is about 490 ms.

### 2.3 Data acquisition

A PXI unit 1033 (National Instruments, NI) equipped with fast (16-bit) multifunction modules (NI PXI 6259 and NI PXI 6608) is used to control the gate of the PMTs, the 20 acquisition of the PMT signals and their digitalization (Dari-Salisburgo et al., 2009). A C-RIO (NI model 9002) is mainly dedicated to the control of the inlet box. It includes a thermocouple module (NI 9211) and analog and digital modules (NI 9263, NI 9474) to control valves, pumps and all the other components of the TD-LIF. The software that controls the instrument and allows periodical calibrations and zeroing is written 25 in LabVIEW (NI), held by a supervision software, written in Lookout (NI), that allows on-line historical data trends of all the variables acquired during the measurements.

[Title Page](#)[Abstract](#)[Introduction](#)[Conclusions](#)[References](#)[Tables](#)[Figures](#)[|◀](#)[▶|](#)[◀](#)[▶](#)[Back](#)[Close](#)[Full Screen / Esc](#)[Printer-friendly Version](#)[Interactive Discussion](#)

## 2.4 Data retrieval and calibration

The TD-LIF measures  $\text{NO}_2$  directly and by subtraction organic nitrates and  $\text{HNO}_3$  can be calculated. All the four cells measure  $\text{NO}_2$  concentrations with the following differences: the first, which samples air at ambient temperature gives ambient  $\text{NO}_2$  concentrations, the second cell that samples air heated to temperatures between 150 and 250 °C measures ambient  $\text{NO}_2$  plus the  $\text{NO}_2$  generated from the thermal dissociation of  $\sum\text{PNs}$ , the third cell, since sample air is heated in the inlet channel to temperatures between 350 and 450 °C, detects ambient  $\text{NO}_2$  plus the  $\text{NO}_2$  generated from the thermal dissociation of  $\sum\text{PNs}$  and  $\sum\text{ANs}$ , and finally the last cell samples air heated to more than 550 °C and so measures ambient  $\text{NO}_2$  plus the  $\text{NO}_2$  generated from the thermal dissociation of  $\sum\text{PNs}$ ,  $\sum\text{ANs}$  and  $\text{HNO}_3$ . The concentrations of  $\sum\text{PNs}$  are calculated by subtracting the  $\text{NO}_2$  measured in the second cell from that of the first cell,  $\sum\text{ANs}$  concentrations by subtracting the  $\text{NO}_2$  measured in the third cell from that of the second cell and  $\text{HNO}_3$  concentrations are calculated by subtracting the  $\text{NO}_2$  measured in the fourth cell from that of the third cell. Since organic nitrates and  $\text{HNO}_3$  are calculated as the difference between the total  $\text{NO}_2$  observed by each cell and that of the colder one, an intercomparison between cells was performed to check if there is a substantial difference in the behavior of each cell because the detection limit and accuracy of the measurements of the dissociated compounds depends on the detection limit and accuracy of the  $\text{NO}_2$  measured by every cell. Figure 4 shows the intercomparison of the second, third and fourth cells with the first one when a known amount of  $\text{NO}_2$  is sampled by the common manifold. As expected the performance decreases from the second to the fourth cell since the laser energy decreases and its divergence increases, but all of them show a slope very close to unity and a bias that goes from 29 to 92 ppt. The detection limits are: 9.8 pptv, 18.4 pptv, 28.1 pptv and 49.7 pptv (1 s,  $S/N = 2$ ) for detection of  $\text{NO}_2$  by the  $\text{NO}_2$  cell,  $\sum\text{PNs}$  cell,  $\sum\text{ANs}$  cell and  $\text{HNO}_3$  cell, respectively. The accuracy depends on the uncertainty of the standards and mass flow controller used for the calibration and in this configuration is 10 %, 22 %, 34 % and 46 %

[Title Page](#)[Abstract](#)[Introduction](#)[Conclusions](#)[References](#)[Tables](#)[Figures](#)[◀](#)[▶](#)[◀](#)[▶](#)[Back](#)[Close](#)[Full Screen / Esc](#)[Printer-friendly Version](#)[Interactive Discussion](#)

for  $\text{NO}_2$  cell,  $\sum\text{PNs}$  cell,  $\sum\text{ANs}$  cell and  $\text{HNO}_3$  cell, respectively. As mentioned  $\sum\text{PNs}$ ,  $\sum\text{ANs}$  and  $\text{HNO}_3$  are calculated by subtracting the signal of two channels. Therefore the detection limit of each of them depends on the signal and uncertainties of these two channels (Day et al., 2002):

$$^5 (B - A) \pm \left( \sigma_A^2 + \sigma_B^2 \right)^{1/2} \quad (1)$$

where  $A$  and  $B$  are the signals from adjacent channels ( $\text{NO}_2$  cell and  $\sum\text{PNs}$  cell to retrieve  $\sum\text{PNs}$  concentrations or  $\sum\text{PNs}$  cell and  $\sum\text{ANs}$  cell to calculate  $\sum\text{ANs}$  concentrations) and  $\sigma$  is the associated uncertainties in each channel. For example for about 90 pptv of background  $\text{NO}_2$  the detection limit of  $\sum\text{PNs}$  is 120 pptv (10 s,  $S/N = 2$ ), for about 300 pptv of background  $\sum\text{PNs}$  it is 240 pptv (10 s,  $S/N = 2$ ) for  $\sum\text{ANs}$  and for about 70 pptv of background  $\sum\text{ANs}$  it is 420 pptv (10 s,  $S/N = 2$ ) for  $\text{HNO}_3$ .

10 The TD-LIF is routinely calibrated against standard  $\text{NO}_2$  using a cylinder of 5 to 8 ppm of  $\text{NO}_2$  in zero air (SIAD SIT certificate, NIST traceable) diluted in zero air (Dari-Salisburgo et al., 2009). Since all the cells measure  $\text{NO}_2$  they are calibrated 15 only for  $\text{NO}_2$  since in the heated inlets  $\sum\text{PNs}$ ,  $\sum\text{ANs}$  and  $\text{HNO}_3$  achieve a complete dissociation into  $\text{NO}_2$  (Day et al., 2002).

### 3 Results

#### 3.1 Laboratory tests: zeroing and selectivity

Figure 5 shows a time series of  $\text{NO}_2$ , PAN and ethyl nitrates detected by the first three 20 cells of the TD-LIF. A mixture of about 800 pptv of  $\text{NO}_2$ , 3 ppbv of PAN and 4 ppbv of ethyl nitrates was generated in the laboratory and sent to the common inlet, with the  $\sum\text{PNs}$  inlet channel heated at 200 °C, the  $\sum\text{ANs}$  inlet channel at 450 °C and that of  $\text{NO}_2$  at ambient temperature. A high-purity zero air is periodically sent to the common inlet to check if all the cells, including those that sample heated air, reach the zero level.

[Title Page](#)[Abstract](#)[Introduction](#)[Conclusions](#)[References](#)[Tables](#)[Figures](#)[|◀](#)[▶|](#)[◀](#)[▶](#)[Back](#)[Close](#)[Full Screen / Esc](#)[Printer-friendly Version](#)[Interactive Discussion](#)

All the cells go to zero when zero air is sampled with no residue of the organic nitrates and  $\text{NO}_2$  sent previously and they reach zero with no lag-time and all simultaneously.

To determine the response of the TD-LIF as a function of the inlet temperature and its selectivity to separate organic nitrates, a series of experiments were carried out.

5 Figure 6 (upper panel) shows a test where the common inlet sampled a mix of ethyl nitrates and  $\text{NO}_2$  while the temperature of the  $\sum\text{ANs}$  inlet channel was changing from 200 °C to 450 °C and the  $\text{NO}_2$  inlet channel was at ambient temperature. At the beginning about 0.45 ppbv of  $\text{NO}_2$  and 0.5 ppbv of ethyl nitrate were delivered to the common inlet and the temperature of the  $\sum\text{ANs}$  inlet channel was kept at 200 °C, which is the 10 set temperature for the thermal dissociation of  $\sum\text{PNs}$  into  $\text{NO}_2$ . In this first part of the experiment the  $\sum\text{ANs}$  cell measured exactly the same  $\text{NO}_2$  concentration observed by the  $\text{NO}_2$  cell even if it was sampling 0.5 ppbv of ethyl nitrate. This gives two insights: 15 (1) at the temperature of  $\sum\text{PN}$  thermal dissociation, ethyl nitrate, which is one of the  $\sum\text{ANs}$ , is not dissociated into  $\text{NO}_2$ , therefore the  $\sum\text{PNs}$  channel does not suffer interference due to the presence of ethyl nitrate and since all the ANs compounds have the same dissociation temperature of ethyl nitrate it does not suffer interference due to the presence of  $\sum\text{ANs}$  (Day et al., 2002), (2) the  $\sum\text{ANs}$  channel when not heated to the right temperature to dissociate  $\sum\text{ANs}$  measures only ambient  $\text{NO}_2$  and at exactly the same concentrations detected by the cell that samples from the inlet at ambient temperature without bias or interferences due to the presence of one AN. After some time 20 sampling with the  $\sum\text{ANs}$  inlet channel kept at 200 °C, this temperature was increased up to 450 °C, and kept at this temperature for a while. As the temperature rose the  $\text{NO}_2$  concentration detected by the  $\sum\text{ANs}$  cell increased and when the heater temperature reached 450 °C the cell detected about 0.9 ppbv of  $\text{NO}_2$ , from the background  $\text{NO}_2$  25 sent to the inlet plus that converted from 0.5 ppbv of ethyl nitrate. Later, after switching off the heater, the temperature of the  $\sum\text{ANs}$  inlet channel dropped back to 200 °C and again the  $\sum\text{ANs}$  cell detected the same amount of  $\text{NO}_2$  as measured by the first cell. At around time 343.52 (day of the year) the amount of ethyl nitrate was doubled and the temperature of the  $\sum\text{ANs}$  inlet channel rose again to 450 °C. At this temperature,

[Title Page](#)

[Abstract](#)

[Introduction](#)

[Conclusions](#)

[References](#)

[Tables](#)

[Figures](#)

◀

▶

◀

▶

[Back](#)

[Close](#)

[Full Screen / Esc](#)

[Printer-friendly Version](#)

[Interactive Discussion](#)



as expected, the  $\sum$ ANs cell measured the  $\text{NO}_2$  sent plus two times the previous  $\text{NO}_2$  measured due to the dissociation of twice the concentration of ethyl nitrate. Also in this situation, when the heater of the  $\sum$ ANs inlet channel was switched off the  $\sum$ ANs cell detected the same amount of  $\text{NO}_2$  as measured by the  $\text{NO}_2$  cell. Figure 6 (lower panel) shows another experiment to further check the selectivity of the TD-LIF. During this test a synthetic mixture of about 0.9 ppbv of PAN and 2.4 ppbv of ethyl nitrate was supplied to the common inlet of the TD-LIF. The temperature of the  $\sum$ PNs inlet channel was kept at 200 °C for the whole experiment and its cell detected about 0.9 ppbv with a slight decline due to a small decrease in the concentration of PAN sent. At the beginning 5 the temperature of the  $\sum$ ANs inlet channel was kept at 450 °C and, as expected, the  $\sum$ ANs cell detected about 3.3 ppbv of  $\text{NO}_2$  that was the result of the thermal dissociation of 0.9 ppbv of PAN and 2.4 ppbv of ethyl nitrate. Later, reducing the temperature 10 of the  $\sum$ ANs inlet channel from 450 °C to 200 °C, the  $\sum$ ANs cell detected exactly the same concentrations as the  $\sum$ PNs cell. This experiment was concluded with another 15 rise and drop of the  $\sum$ ANs inlet channel to confirm again that at 450 °C the  $\sum$ ANs cell measured PAN plus ethyl nitrates, whereas at 200 °C only PAN. This is another proof that the inlet system set at two distinct temperatures is able to separate PAN from ethyl nitrates, and since all the PNs compounds have the same dissociation temperature as PAN and all the ANs the same as ethyl nitrate (Day et al., 2002), the TD-LIF can reliably 20 detect  $\sum$ PNs and  $\sum$ ANs.

### 3.2 Laboratory tests: conversion efficiency of ANs and PNs in presence of $\text{NO}_2$

One of the concerns in the detection of organic nitrates by thermal dissociation is the potential recombination of dissociated products could be a possible interference. For example when ANs are thermally dissociated they produce RO and  $\text{NO}_2$ , the latter is detected by the TD-LIF to calculate the amount of ANs, but the first can react with  $\text{NO}_2$  and reproducing ANs. A series of lab tests were performed to check the probability 25 of recombination of dissociated products. Figure 7 shows TD-LIF measurements of the  $\sum$ ANs channel when a laboratory generated mixture of ethyl nitrate and  $\text{NO}_2$  was

[Aircraft TD-LIF](#)

P. Di Carlo et al.

[Title Page](#)

[Abstract](#)

[Introduction](#)

[Conclusions](#)

[References](#)

[Tables](#)

[Figures](#)

◀

▶

◀

▶

[Back](#)

[Close](#)

[Full Screen / Esc](#)

[Printer-friendly Version](#)

[Interactive Discussion](#)



delivered to the TD-LIF inlet. When the initial ethyl nitrate sent was 2.5 ppbv no recombination was observed with  $\text{NO}_2$  concentrations up to 80 ppbv: the slope of the linear fit is 0.0003 which indicates a possible interference of 0.3 pptv per ppbv of  $\text{NO}_2$ , a value well below the detection limit of the system. A similar insignificant recombination effect was observed when the initial ethyl nitrate was about 6.5 ppbv and 11.5 ppbv. Figure 8 shows the  $\sum\text{PNs}$  detected by the cell that sampled air heated at 200 °C when about 2.3 ppbv of PAN was sent to the TD-LIF inlet together with known amounts of  $\text{NO}_2$  that was increased step by step up to 80 ppbv. This experiment was carried out to test if the addition of  $\text{NO}_2$  suppresses the  $\sum\text{PNs}$  concentration due to recombination of  $\text{RO}_2$  and  $\text{NO}_2$ . The linear fit gives a slope of -0.0030 that implies a suppression of  $\sum\text{PNs}$  at the rate of -3 pptv per ppbv of  $\text{NO}_2$  added, which is a small interference and similar to that observed with other TD-LIF and TD-CRDS (Day et al., 2002; Paul et al., 2009).

## 4 Comparison of in-flight measurements of TD-LIF

### 4.1 Nitrogen dioxide: TD-LIF vs chemiluminescence detector

In summer 2010, the TD-LIF was installed for the first time on-board the UK FAAM BAe 146-301 atmospheric research aircraft during the Role of Nighttime Chemistry in Controlling the Oxidising Capacity of the Atmosphere (RONOCO) campaign. RONOCO was a nighttime campaign aimed to study the role of  $\text{NO}_3$  and  $\text{N}_2\text{O}_5$  in the after-dawn chemistry of the atmosphere, with a few flights carried out during the day. The campaign was based at East Midland airport (UK) to study the chemistry over the UK during two periods: July/August 2010 and January 2011, with 25 research flights.

The BAe 146-301 research aircraft was fitted with several instruments to measure trace gas concentrations, aerosol physical and chemical properties and meteorological parameters, among them there was a chemiluminescence (CL) detector which provided measurements of  $\text{NO}_2$  concentrations with a technique completely different from the TD-LIF. The CL detector uses a photolytic converter (blue-light LED, centered

[Title Page](#)[Abstract](#)[Introduction](#)[Conclusions](#)[References](#)[Tables](#)[Figures](#)[|◀](#)[▶|](#)[◀](#)[▶](#)[Back](#)[Close](#)[Full Screen / Esc](#)[Printer-friendly Version](#)[Interactive Discussion](#)

at 395 nm) to convert  $\text{NO}_2$  into NO, whose concentration is monitored via the detection of the  $\text{NO} + \text{O}_3$  chemiluminescence photons (Kley and McFarland, 1980). Several intercomparisons among  $\text{NO}_2$  instruments have been executed in recent years: one very comprehensive, using five different  $\text{NO}_2$  detectors, was carried out in a simulation 5 chamber and showed good agreements between CL detector and some other  $\text{NO}_2$  instruments including a LIF system (Fuchs et al., 2010). The BAe-146 CL system undertook regular in-flight calibrations and its inlet was located on the same side and less than 8 m away from the TD-LIF inlet. The upper panel in Fig. 9 shows the time series 10 of  $\text{NO}_2$  measured by the TD-LIF and by the CL detector during the first flight of the RONOCO campaign in the night of 16/17 July 2010. The TD-LIF and CL data were acquired with 0.1 s and 1 s integration time respectively, but to compare at the same time 15 frequency the TD-LIF data have been averaged over 1 s intervals. The upper panel in Fig. 9 shows that during the whole flight the two instruments detected very similar amounts of  $\text{NO}_2$  and they tracked the same  $\text{NO}_2$  variability. The lower panel of Fig. 9 shows the scatter plot of the  $\text{NO}_2$  concentration from TD-LIF against that from CL for the whole flight. The correlation between the data observed by the two instruments is robust ( $R^2 = 0.995$ ), a slope very close to unity (1.09) and a small intercept (0.22 ppb). This excellent agreement between TD-LIF and an independent and established 20 system like CL validates the TD-LIF system and shows that it can be effectively used in airborne observations.

#### 4.2 Peroxy nitrates: TD-LIF measurements of $\sum\text{PNs}$ vs BBCEAS measurements of $\text{N}_2\text{O}_5$

Another new system developed by Jones's group in Cambridge (UK), using a well-established technique to observe  $\text{NO}_3$  and  $\text{N}_2\text{O}_5$  (Kennedy et al., 2011), was deployed 25 on the BAe 146-301 aircraft during the RONOCO campaigns. This new system uses broadband cavity enhanced absorption spectroscopy (BBCEAS) to measure  $\text{N}_2\text{O}_5$ , which is one of the  $\sum\text{PNs}$  and in particular the dominant one during nighttime (Day et al., 2002). Therefore even if  $\sum\text{PNs}$  include other nitrates compounds and their

[Title Page](#)[Abstract](#)[Introduction](#)[Conclusions](#)[References](#)[Tables](#)[Figures](#)[|◀](#)[▶|](#)[◀](#)[▶](#)[Back](#)[Close](#)[Full Screen / Esc](#)[Printer-friendly Version](#)[Interactive Discussion](#)

concentrations are usually higher than  $\text{N}_2\text{O}_5$ , a comparison between the TD-LIF and the BBCEAS serves as a good test of the performance of the first instrument at least when  $\sum\text{PNs}$  are dominated by  $\text{N}_2\text{O}_5$ , for instance during nighttime. The upper panel of Fig. 10 shows  $\sum\text{PNs}$  measured by the TD-LIF and  $\text{N}_2\text{O}_5$  detected by the BBCEAS during the second flight of the RONOCO campaign on the night of 17/18 July 2010. The TD-LIF and BBCEAS data were acquired with 0.1 s and 0.4 s integration time respectively, but for the comparison in this figure they have been averaged over 30 s intervals. The upper panel in Fig. 10 shows that in the part of the flight reported here when  $\sum\text{PNs}$  were dominated by  $\text{N}_2\text{O}_5$ , the two instruments detected very similar concentrations and they tracked the same  $\text{N}_2\text{O}_5$  variability. The lower panel of Fig. 10 shows the scatter plot of the TD-LIF and BBCEAS for the same flight reported in the upper panel of Fig. 10. This agreement between TD-LIF measurements and an independent and established technique like BBCEAS is very good: the correlation between the data observed by the two instruments is quite strong ( $R^2 = 0.896$ ), the slope is 0.78 and there is a very small intercept (0.009 ppb). This intercomparison confirms the consistency of the  $\sum\text{PNs}$  measurements and that the TD-LIF can be efficiently used in airborne observations.

## 5 Conclusions

A TD-LIF system for simultaneous measurements of  $\text{NO}_2$ ,  $\sum\text{PNs}$ ,  $\sum\text{ANs}$  and  $\text{HNO}_3$  was built and, after laboratory tests, installed on the UK research aircraft BAe 146-301. The system shows low detection limits for  $\text{NO}_2$  and organic nitrates, which allows observations in different environments. Laboratory tests show the selectivity of the TD-LIF for the detection of organic nitrates and  $\text{HNO}_3$ . Experiments to identify possible interference due to the recombination of thermal dissociation products show an insignificant effect on the  $\sum\text{ANs}$  detection and a very small effect in the  $\sum\text{PNs}$ . To date the TD-LIF has been successfully operated in five field campaigns. In-flight intercomparison of  $\text{NO}_2$  measurements between the TD-LIF and a chemiluminescence system shows an

[Title Page](#)  
[Abstract](#) [Introduction](#)  
[Conclusions](#) [References](#)  
[Tables](#) [Figures](#)  
[◀](#) [▶](#)  
[◀](#) [▶](#)  
[Back](#) [Close](#)  
[Full Screen / Esc](#)

[Printer-friendly Version](#)  
[Interactive Discussion](#)



excellent agreement. Comparison of in-flight measurements of  $\Sigma$ PNs measured by the TD-LIF and  $\text{N}_2\text{O}_5$  measured by a BBCEAS system installed on the same aircraft also show a good agreement. TD-LIF has demonstrated that it is not only robust enough for in-flight observations but also sensitive enough to provide accurate measurements of  $\text{NO}_2$  and organic nitrates.

**Acknowledgements.** This work was performed within the RONOCO consortium supported by the Natural Environmental Research Council (NERC) (University of Cambridge grant award reference RG50086 MAAG/606, University of Leicester grant award reference NE/F006761/1, University of East Anglia grant award reference NE/F005520/1). We acknowledge Ron Cohen and Paul Wooldridge (University of California, Berkeley) for their advice on the design of the TD-LIF. We thank Francesco Del Grande (University of L'Aquila, Italy) for the building of the mechanical parts of the TD-LIF. We thank the BAe-146 pilots and all the people from FAAM, Avalon Aero and DirectFlight for their help during RONOCO campaign. PDC works are supported by Fondazione CarispAQ.

## 15 References

Blake, N. J., Blake, D. R., Swanson, A. L., Atlas, E., Flocke, F., and Rowland, F. S.: Latitudinal, vertical, and seasonal variations of C1-C4 alkyl nitrates in the troposphere over the Pacific Ocean during PEM-Tropics A and B: oceanic and continental sources, *J. Geophys. Res.*, 108, 8242, doi:10.1029/2001JD001444, 2003.

20 Chuck, A. L., Turner, S. M., and Liss, P. S.: Direct evidence for a marine source of C1 and C2 alkyl nitrates, *Science*, 297, 1151–1154, 2002.

Dari-Salisburgo, C., Di Carlo, P., Giammaria, F., Kajii, Y., and D'Altorio A.: Laser induced fluorescence instrument for  $\text{NO}_2$  measurements: observations at a central Italy background site, *Atmos. Environ.*, 43, 970–977, 2008.

25 Day, D. A., Wooldridge, P. J., Dillon, M. B., Thornton, J. A., and Cohen R. C.: A thermal dissociation laser-induced fluorescence instrument for in situ detection of  $\text{NO}_2$ , peroxy nitrates, alkyl nitrates, and  $\text{HNO}_3$ , *J. Geophys. Res.*, 107, 4046, doi:10.1029/2001JD000779, 2002.

[Title Page](#)

[Abstract](#)

[Introduction](#)

[Conclusions](#)

[References](#)

[Tables](#)

[Figures](#)

◀

▶

◀

▶

[Back](#)

[Close](#)

[Full Screen / Esc](#)

[Printer-friendly Version](#)

[Interactive Discussion](#)



Farmer, D. K. and Cohen, R. C.: Observations of  $\text{HNO}_3$ ,  $\sum\text{AN}$ ,  $\sum\text{PN}$  and  $\text{NO}_2$  fluxes: evidence for rapid  $\text{HO}_x$  chemistry within a pine forest canopy, *Atmos. Chem. Phys.*, 8, 3899–3917, doi:10.5194/acp-8-3899-2008, 2008.

5 Flocke, F. M., Weinheimer, A. J., Swanson, A. L., Roberts, J. M., Schmitt, R., and Shertz, S.: On the measurement of PANs by gas chromatography and electron capture detection, *J. Atmos. Chem.*, 52, 19–43, 2005.

10 Fuchs, H., Ball, S. M., Bohn, B., Brauers, T., Cohen, R. C., Dorn, H.-P., Dubé, W. P., Fry, J. L., Häseler, R., Heitmann, U., Jones, R. L., Kleffmann, J., Mentel, T. F., Müsgen, P., Rohrer, F., Rollins, A. W., Ruth, A. A., Kiendler-Scharr, A., Schlosser, E., Shillings, A. J. L., Tillmann, R., Varma, R. M., Venables, D. S., Villena Tapia, G., Wahner, A., Wegener, R., Wooldridge, P. J., and Brown, S. S.: Intercomparison of measurements of  $\text{NO}_2$  concentrations in the atmosphere simulation chamber SAPHIR during the NO3Comp campaign, *Atmos. Meas. Tech.*, 3, 21–37, doi:10.5194/amt-3-21-2010, 2010.

15 Hao, C. S., Shepson, P. B., Drummond, J. W., and Muthuramu, K.: Gas-chromatographic detector for selective and sensitive detection of atmospheric organic nitrates, *Anal. Chem.*, 66, 3737–3743, 1994.

20 Kennedy, O. J., Ouyang, B., Langridge, J. M., Daniels, M. J. S., Bauguitte, S., Freshwater, R., McLeod, M. W., Ironmonger, C., Sendall, J., Norris, O., Nightingale, R., Ball, S. M., and Jones, R. L.: An aircraft based three channel broadband cavity enhanced absorption spectrometer for simultaneous measurements of  $\text{NO}_3$ ,  $\text{N}_2\text{O}_5$  and  $\text{NO}_2$ , *Atmos. Meas. Tech.*, 4, 1759–1776, doi:10.5194/amt-4-1759-2011, 2011.

Kley, D. and McFarland, M.: Chemiluminescence detector for NO and  $\text{NO}_2$ , *Atmos. Technol.*, 12, 63–69, 1980.

25 Marley, N. A., Gaffney, J. S., White, R. V., Rodriguez-Cuadra, L., Herndon, S. E., Dunlea, E., Volkamer, R. M., Molina, L. T., and Molina, M. J.: Fast gas chromatography with luminol chemiluminescence detection for the simultaneous determination of nitrogen dioxide and peroxyacetyl nitrate in the atmosphere, *Rev. Sci. Instrum.*, 75, 4595–4605, 2004.

30 Matsumoto, J., Hirokawa, J., Akimoto, H., and Kajii, Y.: Direct measurement of  $\text{NO}_2$  in the marine atmosphere by laser-induced fluorescence technique, *Atmos. Environ.*, 35, 2803–2814, 2001.

McKinley J. J. and Merriman, D. C.: Permeation tube sources for internal standards in process samples, *Process. Contr. Qual.*, 8, 69–74, 1996.

[Title Page](#)[Abstract](#)[Introduction](#)[Conclusions](#)[References](#)[Tables](#)[Figures](#)[|◀](#)[▶|](#)[◀](#)[▶](#)[Back](#)[Close](#)[Full Screen / Esc](#)[Printer-friendly Version](#)[Interactive Discussion](#)

Monks, P. S., Granier, C., Fuzzi, S., Stohl, A., Williams, M. L., Akimoto, H., Amanni, M., Baklanov, A., Baltensperger, U., Bey, I., Blake, N., Blake, R. S., Carslaw, K., Cooper, O. R., Dentener, F., Fowler, D., Frakou, E., Frost, G. J., Generoso, S., Ginoux, P., Grewet, V., Guenther, A., Hansson, H. C., Henne, S., Hjorth, J., Hofzumahaus, A., Huntrieser, H., Isaksen, I. S. A., Jenkin, M. E., Kaiser, J., Kanakidou, M., Klimont, Z., Kulmala, M., Laj, P., Lawrence, M. G., Lee, J. D., Liousse, C., Maione, M., McFiggans, G., Metzger, A., Mieville, A., Moussiopoulos, N., Orlando, J. J., O'Dowd, C. D., Palmer, P. I., Parrish, D. D., Petzold, A., Platt, U., Poschl, U., Prevot, A. S. H., Reeves, C. E., Reimann, S., Rudich, Y., Sellegri, K., Steinbrecher, R., Simpson, D., ten Brink, H., Theloke, J., van der Werf, G. R., Vautard, R., Vestreng, V., Vlachokostas, C., and von Glasow, R.: Atmospheric composition change – global and regional air quality, *Atmos. Environ.*, 43, 5268–5350, 2009.

Paul, D., Furgeson, A., and Osthoff, H. D.: Measurements of total peroxy and alkyl nitrate abundances in laboratory-generated gas samples by thermal dissociation cavity ring-down spectroscopy, *Rev. Sci. Instrum.*, 80, 114101–114108, 2009.

Perring, A. E., Bertram, T. H., Wooldridge, P. J., Fried, A., Heikes, B. G., Dibb, J., Crounse, J. D., Wennberg, P. O., Blake, N. J., Blake, D. R., Brune, W. H., Singh, H. B., and Cohen, R. C.: Airborne observations of total RONO<sub>2</sub>: new constraints on the yield and lifetime of isoprene nitrates, *Atmos. Chem. Phys.*, 9, 1451–1463, doi:10.5194/acp-9-1451-2009, 2009.

Reeves, C. E., Slemr, J., Oram, D. E., Worton, D., Penkett, S. A., Stewart, D. J., Purvis, R., Watson, N., Hopkins, J., Lewis, A., Methven, J., Blake, D. R., and Atlas, E.: Alkyl nitrates in outflow from North America over the North Atlantic during Intercontinental Transport of Ozone and Precursors 2004, *J. Geophys. Res.*, 112, D10S37, doi:10.1029/2006JD007567, 2007.

Slusher, D. L., Huey, L. G., Tanner, D. J., Flocke, F. M., and Roberts, J. M.: A thermal dissociation-chemical ionization mass spectrometry (TD-CIMS) technique for the simultaneous measurement of peroxyacetyl nitrates and dinitrogen pentoxide, *J. Geophys. Res.*, 109, D19315, doi:10.1029/2004JD004670, 2004.

Turnipseed, A. A., Huey, L. G., Nemitz, E., Stickel, R., Higgs, J., Tanner, D. J., Slusher, D. L., Sparks, J. P., Flocke, F., and Guenther, A.: Eddy covariance fluxes of peroxyacetyl nitrates (PANs) and NO<sub>y</sub> to a coniferous forest, *J. Geophys. Res.*, 111, D09304, doi:10.1029/2005JD006631, 2006.

[Title Page](#)[Abstract](#)[Introduction](#)[Conclusions](#)[References](#)[Tables](#)[Figures](#)[◀](#)[▶](#)[◀](#)[▶](#)[Back](#)[Close](#)[Full Screen / Esc](#)[Printer-friendly Version](#)[Interactive Discussion](#)

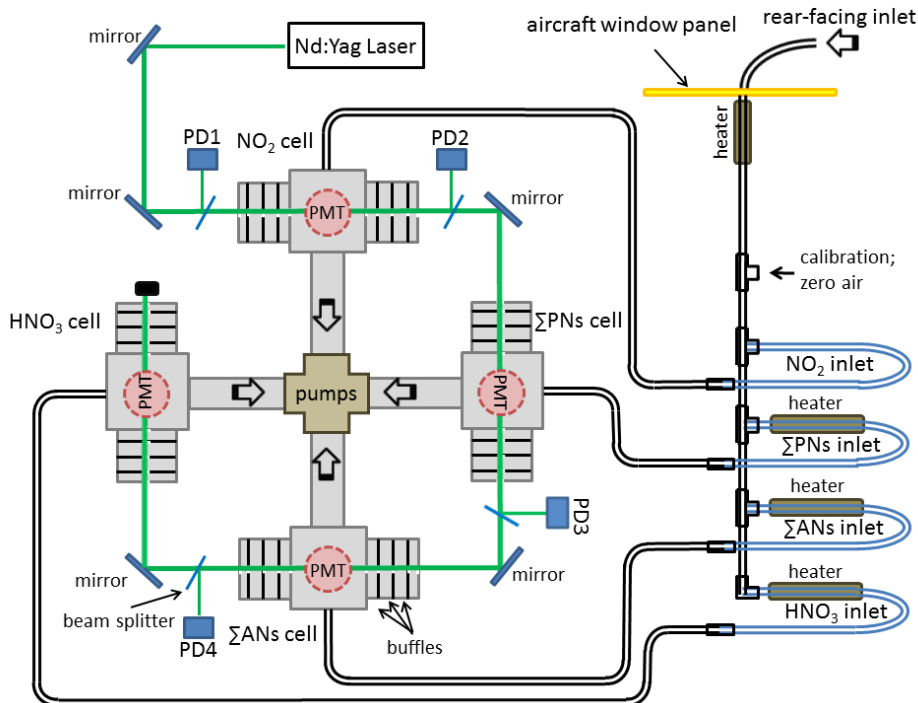


**Fig. 1.** The optical layout of the TD-LIF with schematics of the inlet system. Note that, to simplify the scheme the tube lengths are different here, but in the instrument the length of each of them from the inlet to the detection cell is identical to ensure the same residence time. PD1-PD4 are the four photodiodes monitoring the laser power.

[Title Page](#)[Abstract](#)[Introduction](#)[Conclusions](#)[References](#)[Tables](#)[Figures](#)[|◀](#)[▶|](#)[◀](#)[▶](#)[Back](#)[Close](#)[Full Screen / Esc](#)[Printer-friendly Version](#)[Interactive Discussion](#)

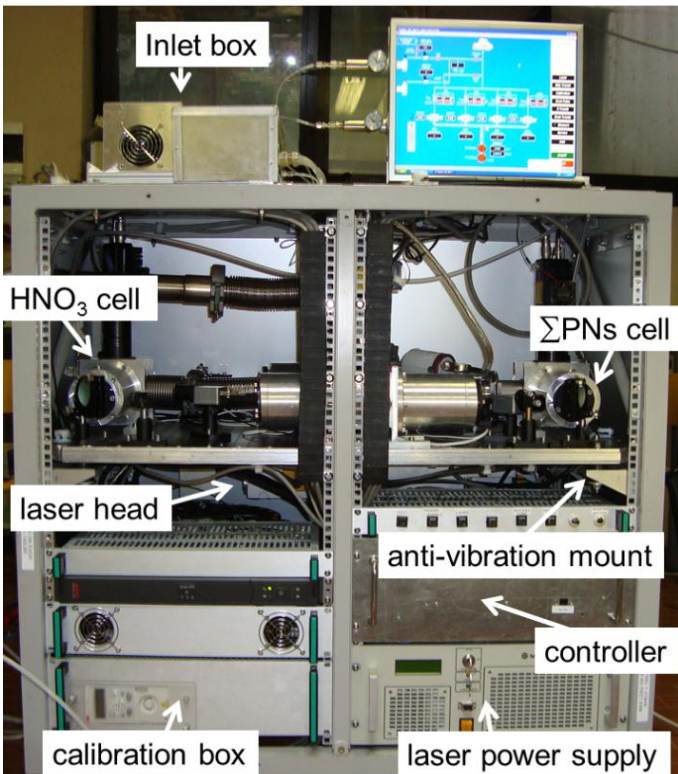


**Fig. 2.** A photograph of the TD-LIF installed in the rack for use on board the FAAM BAe 146-301 research aircraft. The inlet box includes the quartz tubes with heater for thermal dissociation of organic nitrates and  $\text{HNO}_3$  into  $\text{NO}_2$ .

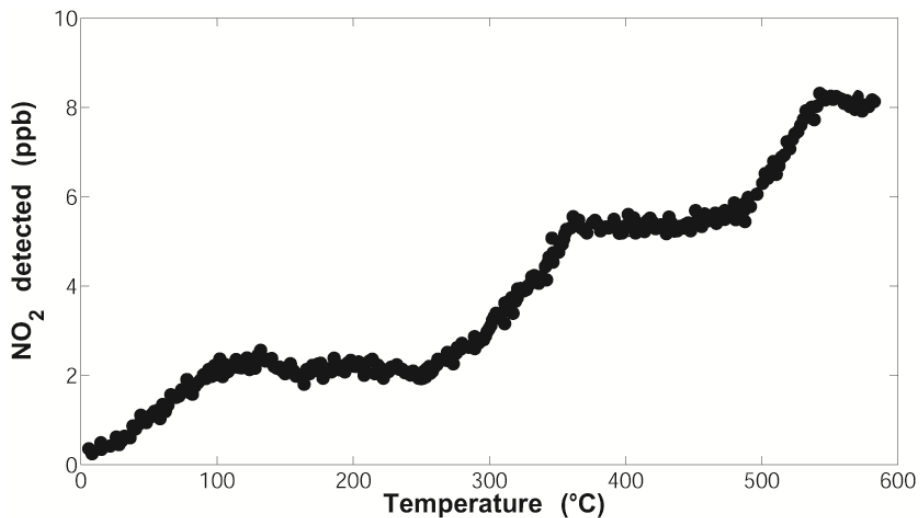


**Fig. 3.** Temperature scan when the TD-LIF sampled synthetic PAN, ethyl nitrates and  $\text{HNO}_3$ , generated in the laboratory to identify the temperatures where these compounds are thermally dissociated into  $\text{NO}_2$ .

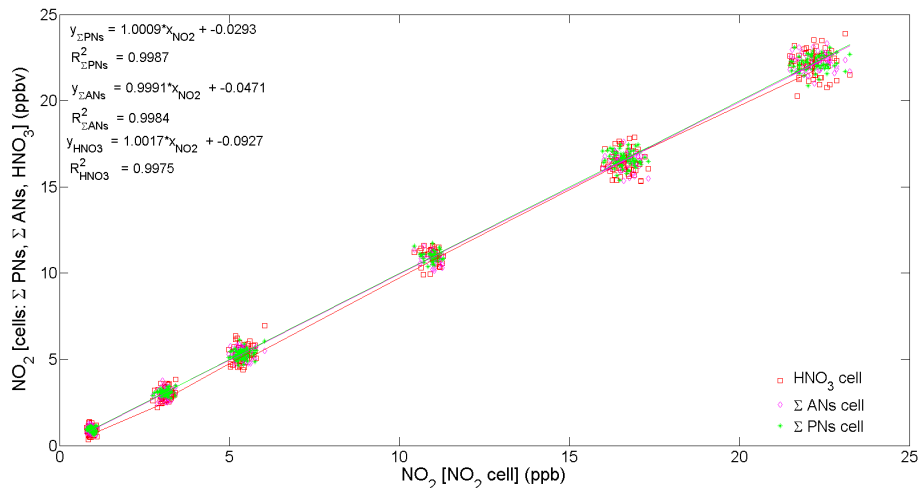


**Fig. 4.** Intercomparison between the first cell and the other three cells when the common inlet sampled different concentrations of  $\text{NO}_2$ , sent using the calibration system of the TD-LIF.

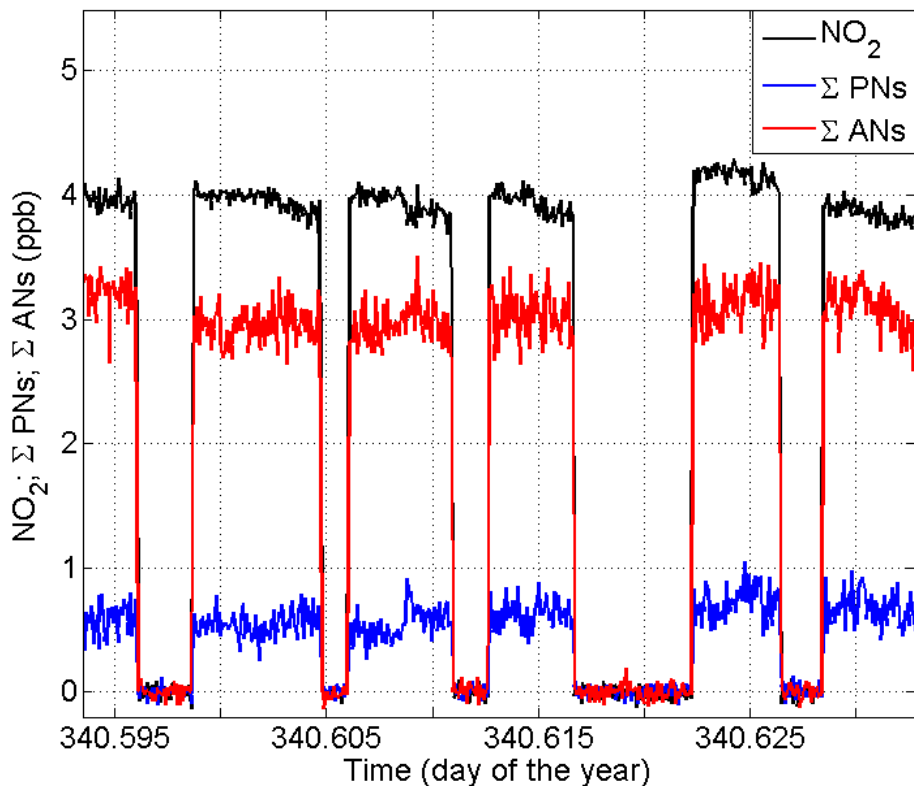


**Fig. 5.** Measurements of a mixture of  $\text{NO}_2$ , PAN and ethyl nitrate with distinct cells of the TD-LIF, generated in a laboratory test. Zero air is sent periodically to check the capability of the system to flush the organic nitrates.

[Title Page](#)[Abstract](#)[Introduction](#)[Conclusions](#)[References](#)[Tables](#)[Figures](#)[|](#)[|](#)[◀](#)[▶](#)[Back](#)[Close](#)[Full Screen / Esc](#)[Printer-friendly Version](#)[Interactive Discussion](#)

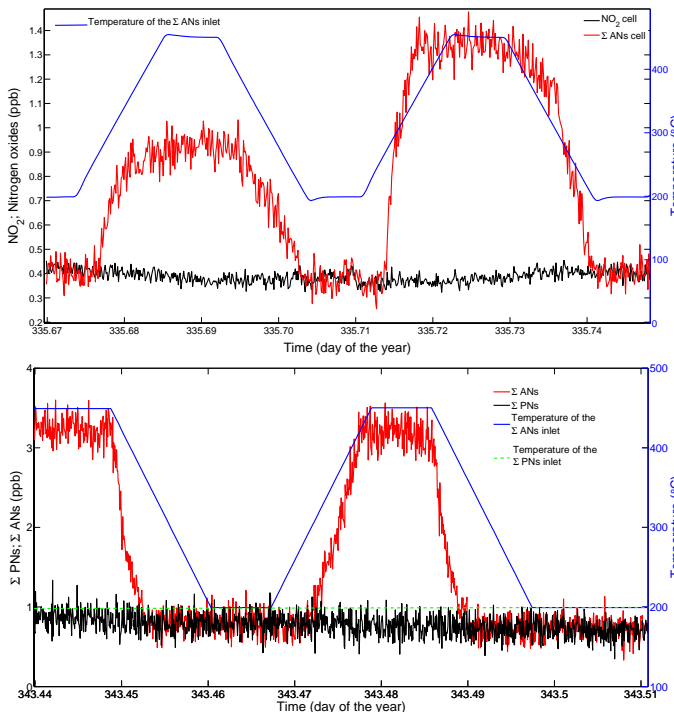


**Fig. 6.** Upper panel: temperature scan of the  $\Sigma$ ANs inlet channel when the TD-LIF sampled a mixture of ethyl nitrate and  $\text{NO}_2$ . After the first temperature scan the concentration of ethyl nitrate was doubled. For all the experiments the  $\text{NO}_2$  cell sampled air at ambient temperature. Lower panel: temperature scan of the  $\Sigma$ ANs inlet channel when the TD-LIF sampled a mixture of ethyl nitrate and PAN. For all the experiment the  $\Sigma$ PNs inlet channel was heated to 200  $^{\circ}\text{C}$  to detect PAN.

Title Page

Abstract

Introduction

Conclusions

References

Tables

Figures

|◀

▶|

◀

▶

Back

Close

Full Screen / Esc

Printer-friendly Version

Interactive Discussion



## Aircraft TD-LIF

P. Di Carlo et al.

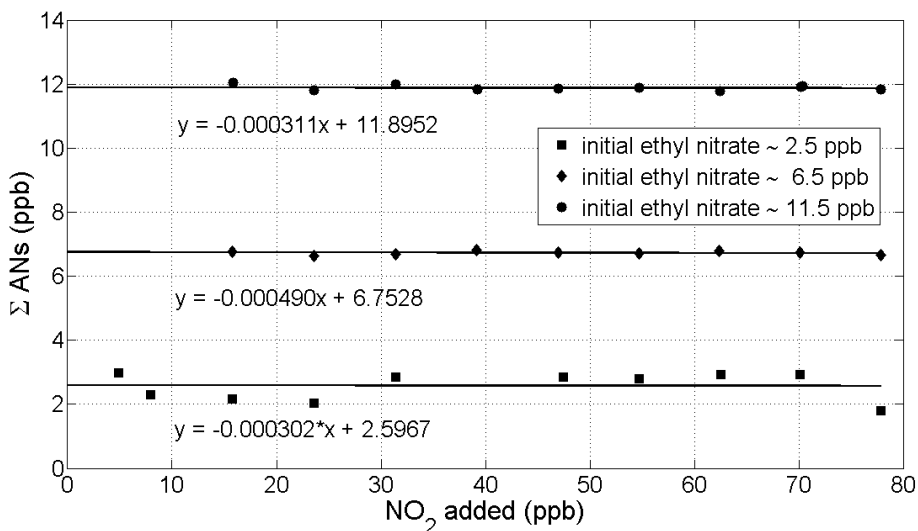


**Fig. 7.** Measurements of  $\Sigma$ ANs when the TD-LIF sampled a mixture of ethyl nitrate and different concentrations of  $\text{NO}_2$  to check for possible interference of the recombination of compounds produced during the dissociation of  $\Sigma$ ANs. This experiment was carried out for different initial concentrations of ethyl nitrate.

Title Page

## Abstract

Introduction

## Conclusion:

References

## Tables

## Figures

1 <

1

Bac

Close

Full Screen / Esc

## Interactive Discussion



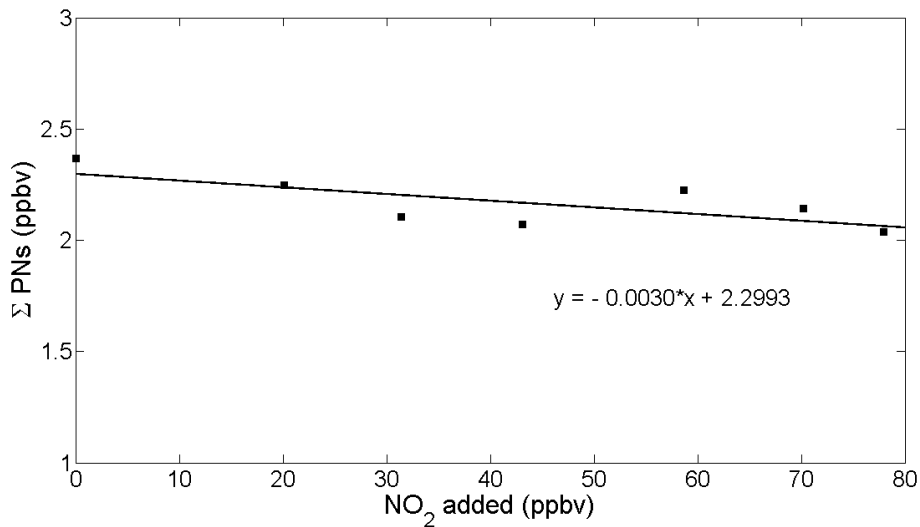


**Fig. 8.** Measurements of  $\Sigma$ PNs when the TD-LIF sampled a mixture of PAN and different concentrations of  $\text{NO}_2$  to check for possible interference due to the recombination of  $\text{RO}_2$  and  $\text{NO}_2$ .

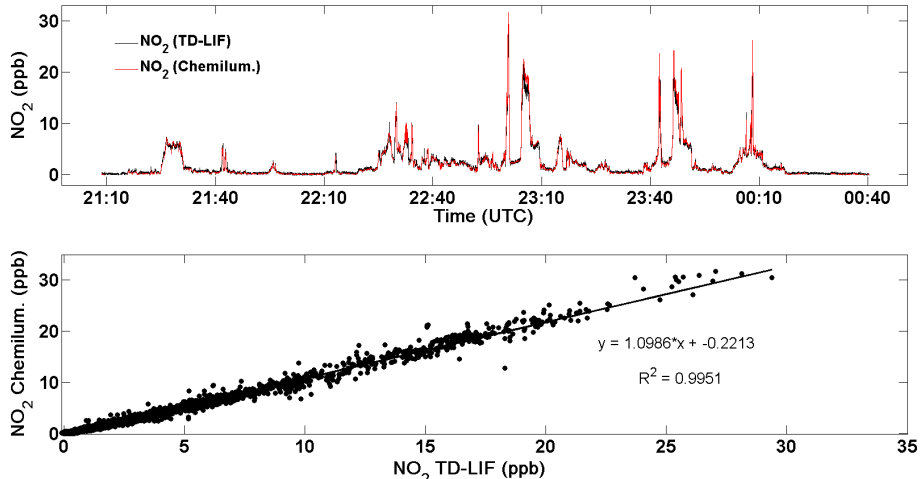


**Fig. 9.** Upper panel: time series of in-flight measurements of  $\text{NO}_2$ , on board the research aircraft BAe 146-301, detected by a chemiluminescence system and by the TD-LIF. Lower panel: scatter plot of  $\text{NO}_2$  measured by a chemiluminescence system and by the TD-LIF reported in the upper plot of this figure.

[Title Page](#)[Abstract](#)[Introduction](#)[Conclusions](#)[References](#)[Tables](#)[Figures](#)[|](#)[|](#)[◀](#)[▶](#)[Back](#)[Close](#)[Full Screen / Esc](#)[Printer-friendly Version](#)[Interactive Discussion](#)

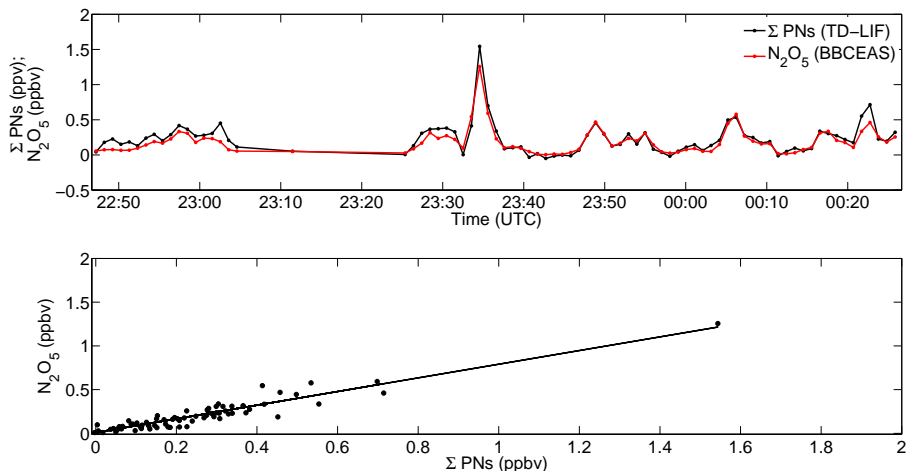


**Fig. 10.** Upper panel: time series of measurements on board the research aircraft BAe 146-301 of  $\Sigma$ PNs and  $\text{N}_2\text{O}_5$  detected by the TD-LIF and by the BBCEAS, respectively. Lower panel: scatter plot of  $\Sigma$ PNs and  $\text{N}_2\text{O}_5$  reported in the upper panel of this figure.

[Title Page](#)[Abstract](#)[Introduction](#)[Conclusions](#)[References](#)[Tables](#)[Figures](#)[|](#)[|](#)[◀](#)[▶](#)[Back](#)[Close](#)[Full Screen / Esc](#)[Printer-friendly Version](#)[Interactive Discussion](#)